A Count-Based Radionuclide Method for Volume Quantitation Using Conjugate Imaging and an External Reference Source: Theoretical Consideration and Phantom Study

Chi-Kwan Yen, Aileen D. Lim and Robert J. Lull

Department of Nuclear Medicine, San Francisco General Hospital, Department of Laboratory Medicine, University of California, San Francisco

A count-based method was developed for ventricular volume determination during multigated equilibrium cardiac blood-pool imaging (MUGA). **Methods:** Two sets of conjugate images of the volume were obtained, one with an external reference overlying the volume and the other without. The reference has known activity and dimension. The ratio of the geometric mean count rates over a pixel obtained from these two conjugate images, $Ratio_{geo}$, and the ratio of the specific activity in the reference to that in the volume, $Ratio_{ext}$, were used to calculate the length of the volume over that pixel perpendicular to the camera face, H, as a function of the length of the reference source, R, and the attenuation coefficient, u_b, of the volume:

$$e^{u_bH/2}-e^{-u_bH/2}=\frac{Ratio_{ext}}{Ratio_{geo}}(1-e^{-u_bR}).$$

Based on H, the volume is then calculated. This method corrects for attenuation directly and determines the volume explicitly. To validate this method, phantom studies are carried out with known volumes of ^{99m}Tc containing saline solutions in situations of variable amount of attenuating medium and background activity. **Results:** In all cases, the calculated volume agrees closely with the actual volume. **Conclusion:** This is an accurate method of volume quantitation that is well suited for determining ventricular volume during MUGA studies.

Key Words: ventricular volume; conjugate imaging; reference source; cardiac blood-pool imaging

J Nucl Med 1994;35:644–651

Left ventricular volume is an important prognostic factor in patients with heart disease (*1–5*). It can be measured from multigated equilibrium blood-pool imaging (MUGA) or by geometric and count-based methods (*6–14*). Count-based methods are independent of geometric assumptions and appear more accurate than geometric methods (*8*). With count-based methods, the detected number of counts from the cardiac blood-pool is correlated with the true counts, which are then used to calculate the true volume. The major potential obstacles to these methods are attenuation effects due to surrounding body tissue and self-attenuation by the ventricle. Methods to correct for attenuation include direct measurement of its effect with a transmission source or indirect determination by estimating the attenuation coefficient and tissue thickness (*6–7,10*). The use of a transmission source is limited by its inability to account for self-attenuation effects and limited strength of the source with resultant poor statistics (*15*). Indirect determination of attenuation is hampered by difficulty in estimating relevant parameters (*16–20*).

The purpose of this article is to describe a method of volume determination which utilizes data from an external reference source to account for both of these attenuation effects directly. Two steps are involved. First, two sets of conjugate images are obtained, one with the reference source overlying the volume of interest and the other without. Based on these data, the length perpendicular to the camera face of a pixel (or a group of pixels with similar count rates) in the volume is derived explicitly. Second, the volume is obtained based on this length. These steps, as well as potential confounding factors, are described below. The procedure is easily automated and is quite suitable for clinical studies.

THEORY

Calculating Length of the Volume Perpendicular to the Camera Face

The configuration under consideration consists of a volume V with uniform radioactivity C_b situated between two nonradioactive attenuating mediums 1 and 2 (Fig. 1). The attenuation coefficient of V is u_b, while that of the attenuating mediums 1 and 2 are u_1 and u_2 respectively. Taking self-attenuation into account, the count rate recorded by a gamma camera with a parallel-hole collimator over a pixel

Received May 4, 1993; revision accepted Jan. 13, 1994.

For correspondence or reprints contact: Chi-Kwan Yen, MD, Department of Nuclear Medicine, San Francisco General Hospital Medical Center, Building 100, Room 157, 1001 Potrero Ave., San Francisco, CA 94110.

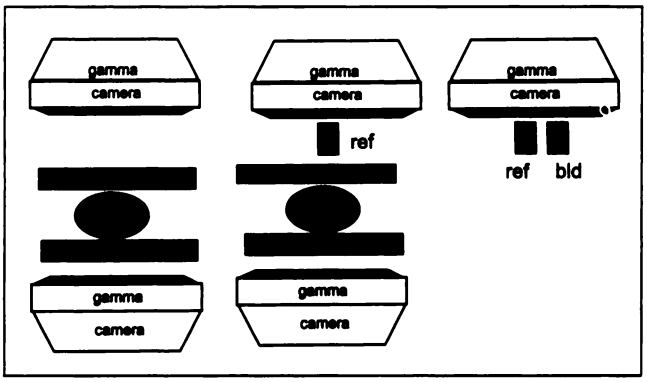

FIGURE 1. Schematic diagram of experimental setup used to quantitate volume (V). V has a specific activity c_b. Reference source (Ref) has height R and specific activity c_R. Conjugate images are first obtained with the volume between attenuating mediums 1 and 2. Conjugate images are then obtained with the Ref placed over the volume. The specific activity in the reference is then related to that in the volume by imaging Ref with a source, bld, having identical geometry but containing specific activity c_b.

(or a group of pixels with similar count rates) P in V with length H perpendicular to the camera face is dependent on C_b, attenuation of photons due to the external mediums and self-attenuation, and the counting efficiency of the gamma camera. With a reference volume (ref) placed over V, the count rate recorded also contains the contribution from this source. Let reference be a rectangle box with length R parallel to H, let $Ratio_{geo}$ denote the ratio of the geometric mean count rate from P to that due to a comparable area in reference and let $Ratio_{ext}$ denote the ratio of specific activity in the reference to that in the volume, an equation is then obtained relating H to R:

$$e^{u_b H/2} - e^{-u_b H/2} = \frac{Ratio_{ext}}{Ratio_{geo}} (1 - e^{-u_b R}). \quad \text{Eq. 1}$$

Note that any attenuation effect due to the external medium is eliminated by using $Ratio_{geo}$ in the equation. The other terms in Equation 1 reflect self-attenuation effects due to reference and volume and an additional term due to reference being attenuated by the ventricle as well. Since all variables in this equation except H are measured, H is obtained explicitly. Derivation of Equation 1 is given in Appendix A.

Calculating Volume

The most direct method to obtain the volume, V, is to calculate H for each pixel, multiply by the area of the pixel and sum over V. However, this requires manipulating data on a pixel-by-pixel basis, which is not currently available on our camera-computer system. Instead, volume is calculated by equating the ratio of the count rates in V (V_{counts}) to that in the hottest pixel (Ant_{max}) with the ratio of the volumes between them:

$$\text{Volume} = \frac{V_{counts}}{Ant_{max}} * H * S^2. \quad \text{Eq. 2}$$

Here the hottest pixel is assumed to have length H and the area of a pixel in the imaging matrix is S^2. If applied directly, this approach introduces a systematic underestimation of the volume due to the difference in self-attenuation between the hottest pixel and the rest of the volume. This effect is dependent on u_b and on both the shape and volume of V. In order to correct for this error, the magnitude of the underestimation is calculated for different volumes of spheres in Appendix B. The results are tabulated (see Table B1) and used to correct for the error in volume determination with Equation 2 above. If necessary, similar calculations can be carried out for different geometric configurations.

Potential Confounding Factors

The major assumption of the proposed method is that geometric mean count rates are independent of the location of the radioactive source. This assumption can be evaluated by measuring camera sensitivity as a function of the distance between the source and camera face. Other factors affecting the proposed approach include the effects of background activity, thickness of attenuating medium and ambiguity in the assignment of regions of interest (ROIs) (*15,18*).

Effect of Camera Sensitivity with Distance

In addition to its intrinsic properties, the sensitivity of the gamma camera is dependent on the properties of the collimator and the presence of Compton scatter. These factors lead to a change in count rate with distance (*7,18,21,22*). They are minimized by using a high-resolution collimator, narrowing the energy window to 5% and the use of background subtraction (*15*). Empirically, count rate as a function of depth will be determined and used to correct for this potential source of error.

Effect of Background Activity

Background activity is usually present clinically. Although no perfect procedure exists to account for this effect, the use of background subtraction partially corrects for this source of error. Background subtraction also partially accounts for scatter effect. In this study, ROI background is drawn manually as a crescent close to the volume. The effectiveness of this approach will be determined by carrying out volume determination with increasing background activity levels.

Effect of Thickness on Attenuating Medium

Increasing attenuating medium thickness decreases true count rate and increases Compton scatter count rate. In our proposed method, the count rate from reference is compared with those from volume. Since attenuation and Compton scattering effects are comparable for these two sources, they are not expected to significantly affect our method.

ROI Assignment

The apparent size of a source increases with its distance from the camera face (*18*), which with the presence of background activity, leads to ambiguity in ROI assign-

ment. To ensure uniformity in data processing, a 10% threshold defined as background activity plus 10% of the difference between the per pixel peak count rate in volume and background is used to determine ROIs for the volume on the image with the source closest to the camera. On the same image, the ROI for the hottest pixels is drawn. The mirror image of this ROI is then used to obtain count rates for the hottest pixels on the conjugate image.

MATERIALS AND METHODS

Experimental Setup

A flask is filled with normal saline to which enough ^{99m}Tc is added to yield a specific activity of around 5 μCi/cc. The contents of this flask are used to fill phantoms whose length and/or volume are to be determined.

The experimental setup is designed to simulate the actual situation in the chest. A phantom simulating the ventricle is viewed by the gamma camera in opposite directions. The chest wall is simulated by placing two attenuating mediums between the ventricle and the camera. These mediums consist of books, which have attenuation coefficients similar to body tissue and are readily available in different thicknesses. The presence of lung tissue with the attenuating coefficient close to the air is simulated by placing the ventricular phantom at a distance from the attenuating mediums to allow air-space between them. The schematics of the setup is shown in Figure 1.

The reference source is required to have a uniform length perpendicular to the camera face. In the present study, the reference source consists of a beaker containing ~10 mCi of ^{99m}Tc and filled with normal saline to a predetermined height. The beaker measures 3 cm in diameter and is filled to a height of ~3–4 cm. In order to compare the activity in the reference with that in the phantoms, a second identical beaker (BLD) is filled to the same height as that of the reference with the content of the flask. Since these two beakers have identical geometry, by imaging them together, the specific activity of the reference can be related to that of the phantoms. In clinical situations, the use of rectangular closed containers with dimensions comparable to the beakers we used (i.e., 3 × 3 × 3 cm) for both reference and BLD would be more appropriate to prevent content leakage. The BLD content would consist of a known volume of a blood sample taken from the patient. A known amount of saline would be added to fill the container while the reference would be filled with a known volume of saline and a predetermined amount of radioactivity. With the proposed method, only the length of the hottest pixel is to be determined. This cubic reference volume would easily cover the center of the left ventricle in patients. It can be easily positioned over the hottest pixel by viewing the latter on the persistence scope.

In the present study, reference imaging is performed with the phantom already in place. This corresponds to clinical situations for imaging the heart after blood-pool labeling. More accurate results are obtained if reference imaging is performed prior to having the phantom in place. In clinical situations, however, this would result in increased study time and potential misalignment problems. Our approach is designed to closely approximate realistic clinical situations rather than try to obtain a better result by performing reference imaging without the phantom in place.

Two types of phantoms are used. The first consists of different sized beakers. This type of phantom has uniform length and is used to evaluate accuracy of both length and volume determination. The second type of phantom consists of different sized balloons. This type of phantom more closely resembles the shape of the left ventricle and is used to evaluate the accuracy of volume determination.

The phantom is placed between nonradioactive attenuation mediums 1 and 2 of different relative and total thicknesses. Conjugate images are obtained with and without the reference placed above medium 1 overlying the volume.

The background level is simulated by placing a basin on one side of the phantom and sequentially adding predetermined amount of radioactivity.

Data Acquisition and Analysis

Imaging Parameters. Images are acquired on a large field of view gamma camera equipped with a low-energy high-resolution collimator. A 5% energy window centering on the 140 keV ^{99m}Tc peak is used. Each image is acquired for 5 min in a 128 × 128 word matrix using a standard computer system. A two-time zoom is used.

Effect of Increasing Distance on Camera Sensitivity. Determination of the effect of increasing distance on camera sensitivity and apparent volume size is carried out by imaging a source consisting of 10 mCi of ^{99m}Tc diluted with 150 cc of water in a 250-cc beaker at different distances from the camera face. The distance ranges from directly over the camera face to 67.5 cm from the camera face.

Length and Volume Determination. Length determination is obtained with the beaker phantom only, while volume determination is obtained for both beaker and balloon phantoms. After measuring the height of the solution in reference to obtain R, the following set of images are acquired:

1. An image of the reference volume and an identical volume containing C_b is obtained. A box ROI is drawn in the center of each, and the ratio of the count rates is obtained as $Ratio_{ext}$.
2. An image of V is obtained on the anterior view. Without smoothing, a manual ROI encompassing V is drawn based on 10% thresholding. P, a square ROI either 3 × 3 or 6 × 6 in size, is drawn manually on this image over the hottest pixels. A background ROI is drawn manually as a 1–2-pixel thick crescent at 1–2 pixels away from this ROI. After background subtraction, V_{counts} and Ant_{heart} are obtained from these ROIs.
3. Without moving the camera or V, the reference is placed over V and a second image is obtained. Using the same ROI for P, Ant_{ref} is obtained.
4. The camera is rotated through 180°. Without moving V or the reference, a posterior image of V with reference is obtained. The reference is then removed and a posterior image of V without reference is obtained. Mirror images of the ROIs for P and background on the anterior view are used to obtain both $Post_{heart}$ and $Post_{ref}$.
5. Decay-correction is performed on all data.
6. $Ratio_{geo}$ is obtained as geometric mean count rates based on these data.
7. H is obtained based on Equation 1.
8. Volume of V is obtained based on Equation 2 after error correction with Table B1.

Effect of Increasing Attenuation and Background Level on Volume Determination. The effect of increasing attenuation on volume determination is evaluated by increasing the total thick-

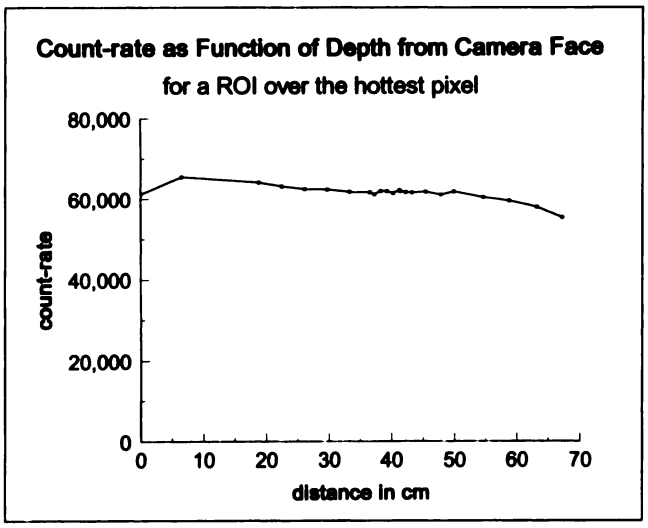

FIGURE 2. Count rate in thousands over a ROI covering the entire volume is plotted as a function of the distance in centimeters between the camera face and the volume.

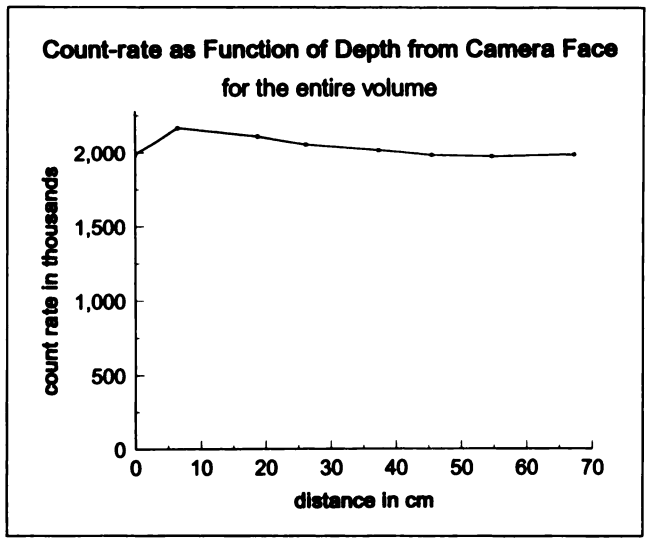

FIGURE 3. Count rate over a ROI placed near the center of the volume is plotted as a function of the distance in centimeters between the camera face and the volume.

ness of attenuating mediums 1 and 2 from 4.8 cm to 19.5 cm. Initially, the effect of asymmetrical attenuating medium on scattering is evaluated to determine whether this would lead to a decrease in the accuracy of our method by varying the relative thickness of attenuation mediums on the two sides of the phantom, i.e., initially with all the attenuating medium to one side of the phantom, and then redistributing the mediums until they are all on the other side of the phantom. No significant differences are seen. Therefore, only one value is given for each total thickness.

The effect of increasing background levels on volume determination is evaluated by adding predetermined amounts of radioactivity to the basin so that it contains from 0 to 6.9 μCi of ^{99m}Tc per cc of normal saline.

RESULTS

Effect of Source Depth on Count Rate

The count rates for the hottest pixel and the total volume change with distance from the camera face. For the hottest pixel, there is an initial increase in count rate with depth. The count rate then stabilizes until a depth of ~50 cm when a steady decrease is observed (Fig. 2). These data are used to correct for changes in count rate with depth for the hottest-pixel. For total volume, a similar pattern is seen except when the effect is much smaller (Fig. 3).

There is an apparent increase in the size of V with depth. Since the ROIs are drawn manually, this apparent change in size cannot be quantified.

Measurement of Length and Volume with Beaker and Balloon Phantoms

The calculated H correlates well with actual H (Fig. 4). In all cases, the error is 5% or less. Since these phantoms have uniform length, the close relationship between calculated H and actual H should lead to a close relationship between calculated volume and actual volume. This is indeed the case and the error is less than 8% in all cases (Fig. 5). The same close relationship is seen for balloon phantoms between calculated and actual volume, with less than 8% error in all cases (Fig. 5).

Effect of Increasing Attenuation and Background Level on Volume Measurement

Volume determination is not affected by increasing the total thickness of the attenuating medium (Table 1). Based on a 200-cc balloon phantom, the errors are within 5% in all cases.

Volume determination is not affected by increasing background activity until it reaches very high levels. Using a 200-cc balloon phantom containing 5 μCi/cc of ^{99m}Tc, the error is less than 5% until the background activity increased to 6.9 μCi/cc when the error is 14% (Table 2).

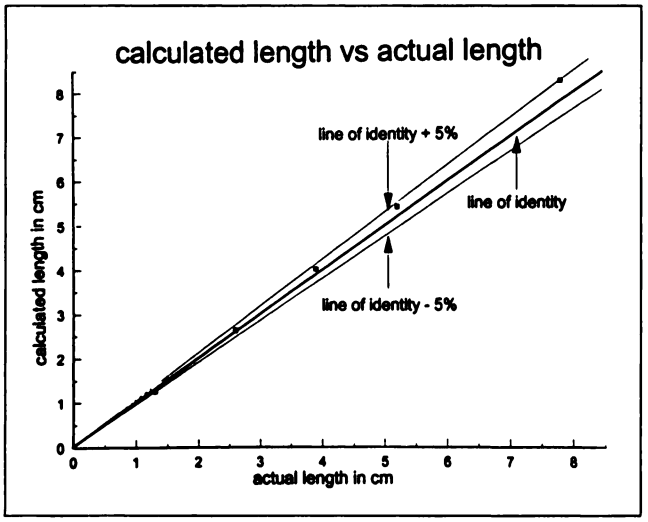

FIGURE 4. Length in centimeters calculated with Equation 1 is plotted against the actual length of beaker phantoms. These phantoms have uniform length. The error is small, within 5% in all cases.

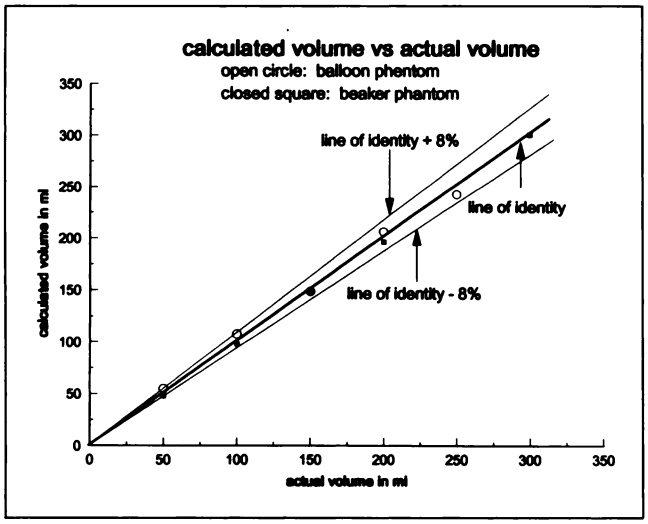

FIGURE 5. Calculated volumes of the beaker (○) and balloon (■) phantoms are compared with the actual volume. The error is small, within 8% in all cases. By combining the two sets of data, the linear regression equation is given by: calculated volume = 2.66 ml + 0.98 × actual volume correlation coefficient is 0.997.

DISCUSSION

In this study, we describe a count-based method which allows for absolute volume quantitation based on comparing the geometric mean count rate from the volume to that obtained from a known reference source situated above the volume. By taking self-attenuation effect into account, an explicit expression for volume is obtained with this method. It is independent of assumptions concerning attenuation effects, size or shape of the volume. Results from phantom studies support its accuracy in volume quantitation. It is well suited for use in conjunction with MUGA studies. We are currently incorporating this method into a routine clinical protocol.

Attenuation correction is the most important factor in a count-based method of volume quantitation (*6,7,9,10*). By directly measuring attenuation, transmission imaging offers a consistent method of accounting for attenuation due to external mediums (*15*). Our method is similar to transmission imaging in that attenuation due to external mediums is directly accounted for since the gamma rays from the reference and ventricular region travel through the same external attenuating mediums. However, transmission imaging does not correct for self-attenuation effects and an explicit expression for volume is obtainable only by assuming that this effect is small or by taking an orthogonal view to estimate the length of the volume. Small volume assumption results in an error which increases with increasing volume and is quite significant in cases of ventricular dilatation (*15*). An orthogonal view measures only the longest length of the ventricle. Since the left ventricle is not rectangular, using the longest length results in an error the magnitude of which depends on both the geometry (i.e., how it differs from a rectangle) and the actual volume of the left ventricle. Our method is different in that it takes the self-attenuation effect directly into account, thus enabling us to obtain pixel volume (or a group of pixels) directly.

The count rates from any distributed source of radioactivity depend on the size, shape and attenuation coefficient of the source. With count-based methods, count rates from a small volume of a blood sample are compared with those from the left ventricle to determine left ventricular volume. Since the left ventricle is different in size and shape from a small blood sample, this approach introduces an error whose magnitude depends on the geometry and attenuation coefficient of the left ventricle. With respect to this error, all count-based methods are dependent on geometric assumptions. Appendix B shows a method for calculating this error magnitude.

Another consideration with count-based methods is the dependence of count rates from a source with distance due to the physical characteristics of the gamma camera-collimator system. When the source is small, as is the case of a small blood sample, variability of count rates with distance is considerable. For a source approximating the size of an adult left ventricle, count rates over the depth usually observed in clinical situations is relatively constant (*21*). Therefore, correction with a single constant is probably adequate. For smaller ventricles, such as those for pediatric patients, a different correction factor (or factors) is probably needed. However, in this case, the distance between the ventricle and the camera is much less than with an adult. Since even a pediatric ventricle is far from being a point source, the count rate variation with distance is expected to be relatively small and correctable within the depth usually encountered in a pediatric patient.

Additional factors affecting the use of any count-based method of volume quantitation are the presence of scatter and background activities (*15,18,21–23*). In this study, we

TABLE 1
Calculated Volume (V_c) of a 200-cc Balloon as a Function of Total Thickness of External Attenuating Medium Compared with Actual Volume (V_a)

	Thickness of attenuating medium (cm)				
	19.5	15.7	11.6	8.1	4.8
V_c	196.0	193.5	188.1	200.1	196.1
V_a	200	200	200	200	200
%Error	−2.0%	−3.2%	−5.9%	0.0%	−2.0%

TABLE 2
Calculated Volume (V_c) of a 200-cc Balloon (ROI) Containing 5.2 μCi/cc of Activity as a Function of Increasing Background (Bkgd) Levels Compared with Actual Volume (V_a)

	Bkgd μCi/cc (or cts ROI/Bkgd)				
	0.0 (33.3)	1.2 (11.6)	2.4 (6.0)	3.6 (4.4)	6.9 (1.7)
V_c	204.4	199.9	196.0	189.4	171.7
V_a	200	200	200	200	200
%Error	+2.2%	0.0%	−2.0%	−5.3%	−14.0%

evaluated the effect of these factors on the accuracy of our method for volume quantitation. Our results indicate that scatter does not adversely impact our approach. This may be due to the use of a 5% energy window and a high-resolution collimator. With the 15%–20% energy window commonly used in clinical imaging, the errors due to these factors may be greater. Our preliminary experience with the clinical study demonstrates that adequate statistics are obtained with a 5% energy window. We are in the process of comparing volume calculations obtained with a 5% energy window with those obtained with a 15% window.

Background subtraction is necessary to account for both background activity and scattering. An ROI placed around the source is routinely used clinically and is the method used here. Our results indicate this approach is adequate for obtaining accurate results. A number of more sophisticated procedures have been advocated to provide better estimation of background activity (*24–25*). They will be evaluated to determine the best procedure for background subtraction in clinical situations.

SUMMARY

We present a count-based radionuclide method for volume quantitation. Phantom studies were performed and attest that the proposed method is accurate under conditions of varying volume, attenuating medium and background levels. Our results indicate this method is potentially useful for left ventricular volume quantitation and can be readily incorporated into routine clinical equilibrium gated cardiac studies.

APPENDIX A: CALCULATING VOLUME PERPENDICULAR LENGTH TO THE CAMERA FACE

Conjugate Imaging Without a Reference Volume

This configuration consists of a volume, V, with uniform radioactivity C_b situated between two nonradioactive attenuating mediums 1 and 2 (Fig. 1). The attenuation coefficient of V is u_b, while that of the attenuating mediums 1 and 2 are u_1 and u_2, respectively. Taking self-attenuation into account, the count rate recorded by the gamma camera on the anterior view with a parallel-hole collimator over a pixel in V with length H perpendicular to the camera face is:

$$Ant_H = \left(\frac{EC_b}{u_b}\right)(1 - e^{-u_bH})e^{-u_1X}, \qquad \text{Eq. A1}$$

where E is the counting efficiency of the gamma camera and X is the length of attenuating medium 1 perpendicular to the camera face. A similar expression ($Post_H$) is obtained for the count rate recorded by the gamma camera after 180° rotation with X replaced by Y, the length of the attenuating medium 2 perpendicular to the camera face. The geometric mean count is:

$$\sqrt{(Ant_H * Post_H)} = \frac{EC_b}{u_b}(1 - e^{-u_bH})e^{-(u_1X + u_2Y)/2}. \qquad \text{Eq. A2}$$

Conjugate Imaging with a Reference Volume

A reference volume with length R, attenuation coefficient u_r, and radioactivity C_r is placed above medium 1 (Fig. 1), R, u_r and C_r are measured directly. Without moving V, the count rate recorded by the gamma camera over P on the conjugate images are respectively:

$$Ant_{ref} = Ant_H * e^{-u_rR} + \frac{EC_r}{u_r}(1 - e^{-u_rR}). \qquad \text{Eq. A3}$$

$$Post_{ref} = Post_H + \left(\frac{EC_r}{u_r}\right)(1 - e^{-u_rR})e^{-(u_1X + u_2Y)}e^{-u_bH}. \qquad \text{Eq. A4}$$

In Equations A3 and A4, the first term after the equal sign is due to V. Net count rate due to reference only is obtained by subtracting this term. Their geometric mean count rate is:

$$\sqrt{(Net_{ant-ref} * Net_{post-ref})} = \left(\frac{EC_r}{u_r}\right) \cdot (1 - e^{-u_rR})e^{-(u_1X + u_2Y)/2}e^{-u_bH/2} \qquad \text{Eq. A5}$$

Derivation of H

The ratio ($Ratio_{geo}$) of these two geometric mean count rates is:

$$Ratio_{geo} = \frac{\sqrt{Net_{Ant-ref} * Net_{Post-ref}}}{\sqrt{Ant_{heart} * Post_{heart}}} = \left(\frac{C_ru_b}{C_bu_r}\right)\left(\frac{1 - e^{-u_rR}}{1 - e^{-u_bH}}\right)e^{-u_bH/2}. \qquad \text{Eq. A6}$$

By imaging the reference and that of an identical volume containing radioactivity C_b with the gamma camera (Fig. 1C), the ratio between their count rates is obtained as:

$$Ratio_{ext} = \frac{Ref_{ext}}{Bld_{ext}} = \left(\frac{C_ru_b}{C_bu_r}\right)\left(\frac{1 - e^{-u_rR}}{1 - e^{-u_bR}}\right). \qquad \text{Eq. A7}$$

These two ratios are combined and rearranged so that terms containing H are moved to the left:

$$e^{u_bH/2} - e^{-u_bH/2} = \frac{Ratio_{ext}}{Ratio_{geo}}(1 - e^{-u_bR}). \qquad \text{Eq. A8}$$

Since u_b and R are measured directly, H is obtained explicitly.

APPENDIX B: ERROR ON VOLUME CALCULATION DUE TO SELF-ATTENUATION BASED ON RELATIVE COUNTS

Volume Calculation Based on Relative Count Rates

The relative count rate method of volume calculation assumes that volume is directly proportional to count rate, i.e., the ratio of the volumes equals the ratio of the count rates. This relationship is used to calculate one volume when another volume and the ratio of their count rates are known. With our method, the height, H, of the hottest pixel is calculated and the total counts V_{counts} as well as the counts in the hottest pixel (Ant_{heart}) are directly measured. With this method, the total volume V is obtained by multiplying the area of a pixel (S^2) by H and the ratio of V_{counts} to Ant_{heart}:

$$Volume = \frac{(V_{counts})}{(Ant_{heart})} * H * S^2. \qquad \text{Eq. B1}$$

S^2 depends on the particular gamma camera and matrix size used to acquire the images.

Correction of Error Due to Self-Attenuation

The use of Equation B1 results in an error caused by omitting self-attenuation. The magnitude of this error can be calculated as follows. Let G be a rod with a unit area, specific activity C_b, attenuation coefficient u_b and length g. Taking self-attenuation into account, the count rate, g_{counts}, recorded by the gamma camera with its face perpendicular to G is given by:

$$g_{counts} = \frac{EC_b}{u}(1 - e^{-ug}), \qquad \text{Eq. B2}$$

where E is the counting efficiency of the camera. Let H be another rod with unit area, C_b, attenuation coefficient u and height h. Its count rate, h_{counts}, is given by Equation B3 with g replaced by h. The assumption that count rates are directly proportional to volumes implies that the volume of g is obtained as:

$$h * \frac{g_{counts}}{h_{counts}}. \qquad \text{Eq. B3}$$

Substituting the expression for g_{counts} and h_{counts} into Equation B3, the volume of G based on the relative count rate method is:

$$h * \frac{1 - e^{-ug}}{1 - e^{-uh}}. \qquad \text{Eq. B4}$$

The difference between the expression above and the true volume of G, namely g, is the error resulting from not accounting for self attenuation.

A similar argument can be used to calculate the error due to an extended source such as a sphere with radius, r. The schema of this calculation are given in Figure B1. Along the perimeter of a circle located at the center of the sphere with radius, r, and lying parallel to the camera face, the length, L, of the sphere perpendicular to the camera face is given by:

$$L = \sqrt{r^2 - n^2}. \qquad \text{Eq. B5}$$

The volume formed along this perimeter with a small thickness, dn, is given by:

$$2 \times \pi \times n \times dn \times (2 \times L). \qquad \text{Eq. B6}$$

Integrating this volume from n = 0 to n = r yields the actual volume of the sphere.

The count rate over the hottest pixel is given by Equation B2 with r substituted for g, while the count rate along the perimeter of the circle is given by the same equation with L substituted for g. Based on the relative count rate method, the volume along the perimeter of the circle with radius n is:

$$2 \times \pi \times n \times dn \times (2 \times r) \times \frac{(1 - e^{-u \times (2 \times L)})}{(1 - e^{-u \times (2 \times r)})}. \qquad \text{Eq. B7}$$

Integrating over n yields the volume of a sphere calculated by using the relative count rate method. The difference between Equation B6 and B7 integrated over n is the error due to using self-attenuation. This error depends on the volume of the sphere and its attenuation coefficient. In order to correct for this error

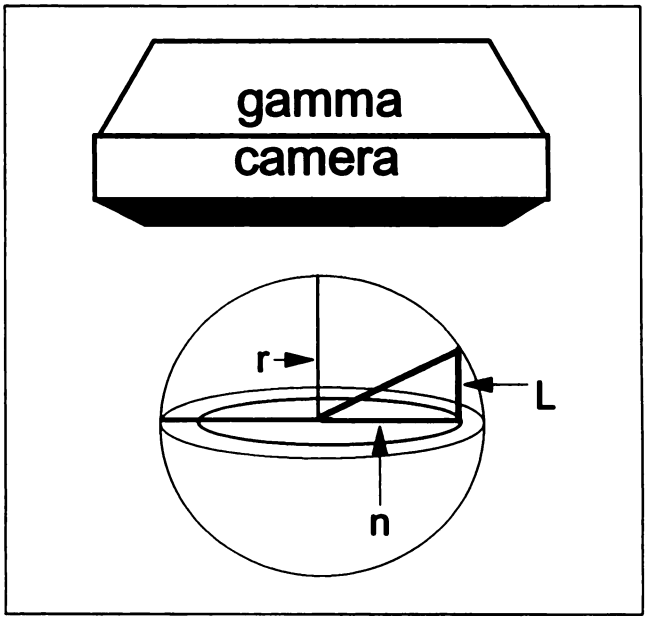

FIGURE B1. Schematic diagram for determining self-attenuation effect for a sphere with radius r. Along the perimeter of a circle with radius n, the length of the sphere perpendicular to the camera face is L. Differences in self-attenuation between L and r is the error associated with ignoring self-attenuation effects along the circle. By integrating this difference from 0 to r, the error for the entire sphere is obtained.

TABLE B1
Volume Calculated Using the Ratio of Total Counts to Counts in the Hottest Pixel Compared with Actual Volume

	Attenuation coefficients				
Actual volume	0.12	0.13	0.14	0.15	0.16
50 ml	53.4	53.6	53.9	54.2	54.4
100 ml	108.4	109.0	109.7	110.4	111.0
150 ml	164.3	165.4	166.6	167.7	168.8
200 ml	220.9	222.5	224.1	225.7	227.3
250 ml	278.0	280.2	282.3	284.4	286.5
300 ml	335.6	338.3	341.0	343.7	346.3
400 ml	451.8	455.8	459.7	463.5	467.3
500 ml	569.4	574.6	579.8	584.8	589.74

A spherical geometry is assumed. The numbers are presented as a function of the volume of the spheres and attenuation coefficients.

source, calculations are made for different radii and attenuation coefficients (Table B1).

If desired, similar calculations can be done to obtain correction factors for geometries other than spheres.

REFERENCES

1. Lamas GA, Pfeffer MA. Left ventricular remodeling after acute myocardial infarction: clinical course and beneficial effects of angiotensin-converting enzyme inhibition. *Am Heart J* 1991;121:1194–1202.
2. Jeremy RW, Allman KC, Bautovitch G, Harris PJ. Patterns of left ventricular dilatation during the six months after myocardial infarction. *J Am Coll Cardiol* 1989;13:304–310.
3. White HD, Norris RM, Brown M, et al. Left ventricular end-systolic volume as the major determinant of survival after recovery from myocardial infarction. *Circulation* 1987;76:44–51.
4. Fuster V, Gersh BJ, Giuliani ER, et al. The natural history of idiopathic dilated cardiomyopathy. *Am J Cardiol* 1981;47:525–521.
5. Hammermeister KE, Chikos PM, Fisher L, et al. Relationship of cardiothoracic ratio and plain film heart volume to late survival. *Circulation* 1979;59: 89–95.
6. Starling MR, Dell'Italia LJ, Nusynowitz ML, et al. Estimates of left-ventricular volumes by equilibrium radionuclide angiography: importance of attenuation correction. *J Nucl Med* 1984;25:14–20.
7. Links JM, Becker LC, Shindledecker JG, et al. Measurement of absolute left ventricular volume from gated blood pool studies. *Circulation* 1982;65: 82–91.
8. Massie BM, Kramer BL, Gertz EW, et al. Radionuclide measurement of left ventricular volume: comparison of geometric and count-based methods. *Circulation* 1982;65:725–730.
9. Burow RD, Wilson MF, Heath PW, et al. Influence of attenuation on radionuclide stroke volume determinations. *J Nucl Med* 1982;23:781–785.
10. Dehmer GJ, Lewis SE, Hillis LD, et al. Nongeometric determination of left ventricular volumes from equilibrium blood pool scans. *Am J Cardiol* 1980; 45:293–300.
11. Slutsky R, Karliner J, Ricci D, et al. Left ventricular volumes by gated equilibrium radionuclide angiography: a new method. *Circulation* 1979;60: 556–564.
12. Sullivan RW, Bergeron DA, Vetter WR, et al. Peripheral venous scintillation angiocardiography in determination of left ventricular volume in man. *Am J Cardiol* 1971;28:563–567.
13. Strauss HW, Zaret BL, Hurley PJ, et al. A scintiphotographic method for measuring left ventricular ejection fraction in man without cardiac catheterization. *Am J Cardiol* 1971;28:575–580.
14. Mullins CB, Mason DT, Ashburn WL, et al. Determination of ventricular volume by radioisotope-angiography. *Am J Cardiol* 1969;24:72–78.
15. Malko JA, Gullberg GT, Kowalsky WP, et al. A count-based algorithm for attenuation-corrected volume determination using data from an external flood source. *J Nucl Med* 1985;26:194–200.
16. Keller AM, Simon TR, Smitherman TC, et al. Direct determination of the attenuation coefficient for radionuclide volume measurement. *J Nucl Med* 1987;28:102–107.
17. Fearnow EC, Jaszczak RJ, Harris CC, et al. Esophageal source measurement of Tc-99m attenuation coefficient for use in left ventricular volume measurement. *Radiology* 1985;157:517–520.
18. Fearnow EC, Stanfield JA, Jaszczak RJ, et al. Factors affecting ventricular volumes determined by a count-based equilibrium method. *J Nucl Med* 1985;26:1042–1047.
19. Schwaiger M, Ratib O, Henze E, et al. Left ventricular volume determinations from radionuclide ventriculogram: the effects of photon attenuation. *Radiology* 1984;153:235–240.
20. Maurer AH, Siegel JA, Denenberg BS, et al. Absolute left ventricular volume from gated blood pool imaging with use of esophageal transmission measurement. *Am J Cardiol* 1983;51:853–858.
21. Myers MJ, Lavender JP, de Oliveira JB, et al. A simplified method of quantitating organ uptake using a gamma camera. *Br J Radiol* 1981;54:1062–1067.
22. Budinger TF. Clinical and research quantitative nuclear medicine system. Symposium on Medical Radioisotope Scintigraphy (IAEA Symposium); October 23–28, 1972:1–62.
23. Gal RA, Grenier RP, Port SC, et al. Left ventricular volume calculation using a count-based ratio method applied to first-pass radionuclide angiography. *J Nucl Med* 1992;33:2124–2132.
24. Goris ML, Daspit SG, McLaughlin P, Kriss JP. Interpolative background subtraction. *J Nucl Med* 1976;17:744–747.
25. Schneider RM, Jaszczak RJ, Coleman RE, et al. Disproportionate effects of regional hypokinesis on radionuclide ejection fraction: compensation using attenuation corrected ventricular volume. *J Nucl Med* 1984;25:747–754.